ELSEVIER

Chemical Geology 236 (2007) 167–179

CHEMICAL GEOLOGY
INCLUDING
ISOTOPE GEOSCIENCE

www.elsevier.com/locate/chemgeo

# Mineralogical and geochemical evidence for coupled bacterial uranium mineralization and hydrocarbon oxidation in the Shashagetai deposit, NW China

Chunfang Cai [a,*], Hailiang Dong [b], Hongtao Li [a], Xinjian Xiao [c], Guanxi Ou [c], Chunming Zhang [d]

[a] *Key Laboratory of Mineral Resources, Institute of Geology and Geophysics, Chinese Academy of Sciences, P.O. Box 9825, Beitucheng Xilu No. 19, Chaoyang District, Beijing 100029, PR China*
[b] *Department of Geology, Miami University, Oxford, OH 45056, USA*
[c] *Beijing Research Institute of Uranium Geology, Beijing 100029, PR China*
[d] *Key Laboratory of Exploration Technologies for Oil and Gas Resources (Yangtze University), Ministry of Education, Jingzhou, Hubei 434023, PR China*

Received 3 May 2006; received in revised form 25 September 2006; accepted 27 September 2006

Editor: P. Deines

**Abstract**

Unusual mineral structures have recently been found in a sandstone-hosted roll-type uranium deposit in the Middle Jurassic Zhiluo Formation in the Shashagetai deposit, the northern Ordos basin, NW China. The structures possess a chemical composition and crystal structure characteristic of mineral coffinite [$(USiO_4)_{1-x}(OH)_{4x}$], which occurs as nanoparticles with size ranging from 5 to 25 nm. These structures are interpreted to be fossilized microorganisms, based on mineralogical biosignatures including morphology, size, occurrence of biogenic coffinite as nano-crystals, and biological elements such as P. The intimate intergrowth of coffinite with secondary pyrite of bacterial origin, as defined by low $\delta^{34}S$ values, and calcite cements with petroleum-derived carbon supports its biogenic origin. Oil inclusions in the host sandstone are characterized by abundant *n*-alkanes, slightly increased $Pr/nC_{17}$ and $Ph/nC_{18}$ ratios, significant amounts of demethylated hopanes and tricyclic terpanes, and the existence of unresolved complex mixtures. These characteristics are interpreted to be a result of mixing of an earlier, heavily degraded oil with a later charged fresh oil; subsequently the oils were slightly degraded. These lines of evidence lead to the proposal that the reduction of sulfate and oxidization of petroleum are likely synchronous with reduction of hexavalent [U(VI)] to tetravalent [U(IV)] uranium by sulfate-reducing bacteria (SRB). The discovery of a natural association of microorganism-like structures, a uranium mineral, and biodegraded petroleum has implications for uranium biomineralization and fossil fuel exploration.


*Keywords:* Uranium deposit; Anaerobic petroleum oxidation; Sulfate-reducing bacteria; Nanoparticle; Microfossil; Sulfur isotopes

* Corresponding author. Tel.: +86 10 62007375; fax: +86 10 62010846.
*E-mail address:* cai_cf@mail.iggcas.ac.cn (C. Cai).

0009-2541/$ - see front matter © 2006 Elsevier B.V. All rights reserved.
doi:10.1016/j.chemgeo.2006.09.007

## 1. Introduction

Microorganisms play important roles in ore formation, cell fossilization and geochemical cycling of metallic elements such as Au, Fe, Mn and U (e.g. Lovley et al., 1991; Watterson, 1991; Reith et al., 2006). Their tolerance and adaptation to toxic and radiation environments bear relevance to the early evolution of life. Uranium biomineralization is currently important for environmental remediation and materials processing industries (Suzuki and Banfield, 1999).

Uranium minerals in sandstone-hosted ore deposits have generally been attributed to U(VI) reduction by biogenic sulfides and organic matter under low temperature conditions (e.g. Rackley, 1972; Reynolds and Goldhaber, 1982). However, such reactions are either too slow or too inefficient as shown by low temperature laboratory experiments (Nakashimima et al., 1984; Lovley and Philips, 1992; Abdelouas et al., 1998). In contrast, iron-reducing and sulfate-reducing bacteria (SRB) have been experimentally shown to be capable of utilizing U (VI) as a preferred electron acceptor for respiration, resulting in reduction of U(VI) to U(IV) directly (Lovley and Philips, 1992; Lovley et al., 1993; Abdelouas et al., 1998). However, there have been only a few studies showing naturally occurring uranium mineralization by microorganisms, largely based on morphological evidence (Milodowski et al., 1990; Min et al., 2005). However, morphology alone is not sufficient to determine biogenicity. Thus, it is necessary to look for other indicators for microbial activity and to determine if geological and environmental conditions are favorable for microorganisms. Recently, new lines of evidence have been presented to determine that some previously determined microbe-like structures are actually biogenic (e.g. Reith et al., 2006; Ueno et al., 2006).

The purpose of this study was to investigate coupled uranium biomineralization and hydrocarbon oxidation in the Shashagetai deposit, NW China. In this paper, microorganism-like structures in the host sandstones of the Middle Jurassic Zhiluo Formation are presented. Multiple approaches were employed to determine if the structures are biogenic. Genetic relationships between anaerobic oxidation of petroleum, sulfate reduction, and uranium (VI) reduction are revealed through an integrated study combining mineralogical and geochemical investigations.

## 2. Geological setting

The Shashagetai sandstone-hosted U-deposit is located in the Yimeng Uplift of the Ordos basin, Northwest China (Fig. 1). The detailed information about the geology and the distribution of oil, gas, and coal in the Ordos basin has been reported elsewhere (Fig. 2, Cai et al., 2005a; Zhang et al., 2006). Briefly, the gas produced in the Paleozoic reservoirs is derived from Ordovician sapropelic to humic–sapropelic organic matter (OM) and Carboniferous–Permian humic OM with a vitrinite reflectance ($R_o$) of 1.4 to 2.2% (Cai et al., 2005a and references therein). The oil produced from the Triassic–Jurassic sequence is derived from Triassic lacustrine algae and terrestrial OM with a $R_o$ range of 0.62 to 1.07% (e.g., Chen and Huang, 1997; Guo et al., 2006). Peak generation of oil and gas took place during the Early to Late Cretaceous (Chen and Huang, 1997; Cai et al., 2005a; Guo et al., 2006). Presently, oil and gas are produced mainly in the Shanbei Slope of the Ordos basin, although commercial oil/gas flows have also recently been found in the Yimeng Uplift (Zhang et al., 2006 and references therein).

The uranium deposit in the study area is hosted by sandstone of braided river facies in the Middle Jurassic Zhiluo Formation (Fig. 2), from which no petroleum has been produced. The host sandstone experienced maximum burial and heating during the end of the Early Cretaceous and had a palaeo-temperature of < 70 °C based

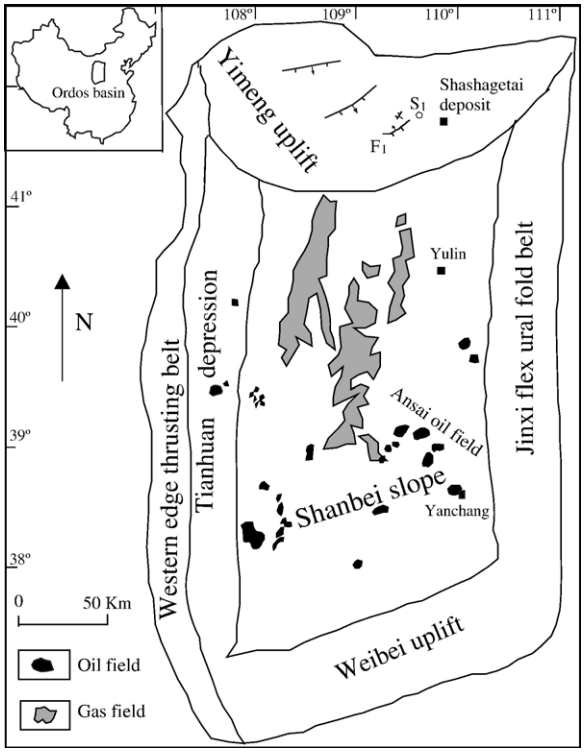


Fig. 1. Map showing the geology and the location of the Shashagetai uranium deposit and the Ansai oilfield, where the studied samples were collected. Well S1 and fault F1 are shown on the map.

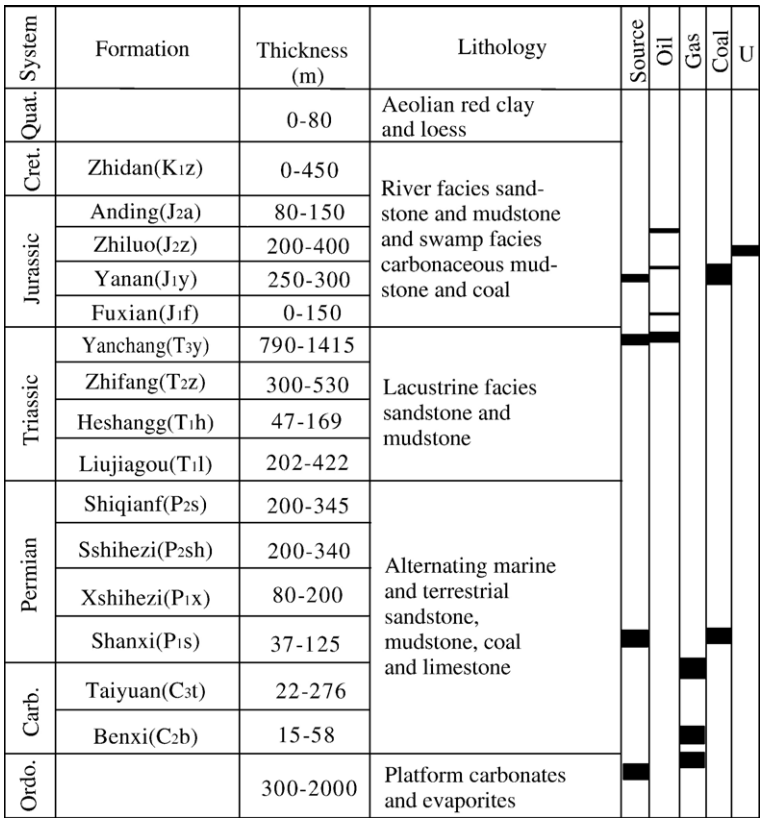


Fig. 2. Stratigraphic column for the Ordos Basin showing petroleum- and U-hosting rock strata.

on a reconstruction of the burial and thermal history on well S1 (Fig. 1, Ren et al., 2006). U(VI) in the host sandstone was mainly supplied by oxidized ground water that was recharged at the outcrop in the north and northwest of the basin. The host sandstone with a higher grade of uranium (>1000 μg/g) is mainly located near the front of the roll-shaped ore body (e.g., at well ZKA 147-39) in the Shashagetai deposit, while on the flanks of the ore body the sandstone has a lower uranium grade. Individual coffinite minerals handpicked from six sandstone samples with a U content higher than 1000 μg/g were measured to have U–Pb ages of 9.8 to 22 Ma ($n=6$) (Xiang et al., 2005).

## 3. Material and methods

### 3.1. Mineralogical and stable isotope analyses

Four outcrop and eighteen well cutting samples were collected from the host sandstone from various depths (Table 1). The uranium content was measured using ICP-MS with a precision of ±8%. Polished thin sections of all the samples listed in Table 1 were examined using an optical microscope. Pyrite was handpicked from 12 selected host sandstone samples for analysis of sulfur isotope using the method reported in Cai et al. (2005b). Pyrite from the selected 12 samples was also examined for microorganism-like structures under a LEO 1450 VP scanning electron microscope (SEM) equipped with an INCA ENERGY 300 X-ray energy dispersive spectroscopy analyzer (EDS) and CHANNEL5 electron backscatter diffraction (EBSD). Samples were either carbon or gold coated and mounted on carbon discs or gold grids. All images were acquired at 20 keV at a working distance of 9 to 11 mm. The beam size was less than 3 nm with a spatial resolution of 1.2 nm. EDS was used to confirm elemental composition for regions of interest. Several samples contained microbe-like structures. One particular sample (from well ZKA147-39 at depth of 180 m, Table 1) with abundant structures was further examined by transmission electron microscopy (TEM) for detailed morphological and compositional analyses. The pyrite (0.43 mm in size) that contains microbe-like structures was recovered from the SEM carbon-disc, broken into pieces, and then examined under H-9000 NAR high-resolution 300 kV TEM. The TEM is equipped with Hitachi SEM/STEM, Philips DX-4 EDS

Table 1
Uranium contents, stable isotopic composition of calcite and pyrite aggregates from Middle Jurassic Zhiluo Formation sandstones

| No. | Well | Depth (m) | $\delta^{13}C$ | $\delta^{18}O$ | $\delta^{34}S$ | U (μg/g) |
|---|---|---|---|---|---|---|
| 52 | SSG-outcrop | 0 | −13.5 | −10.2 | – | – |
| 55 | SSG-outcrop | 0 | −11.5 | −11.2 | – | – |
| 2–34 | SSG-outcrop | 0 | −1.4 | −11.8 | – | 145.4 |
| 2–35 | SSG-outcrop | 0 | −1.7 | −12.6 | – | 262.9 |
| | ZKA0-3-01 | 100.8 | – | – | −36.0 | 1.9 |
| | ZKA3-0-12 | 130.9 | – | – | −39.2 | 37.8 |
| | ZKA3-11-05 | 150.6 | – | – | 15.8 | – |
| | ZKA3-12-01 | 71.9 | – | – | −5.3 | – |
| | ZKA3-12-04 | 103 | – | – | −6.9 | 687.0 |
| 35 | ZKA75-51 | 286 | −8.6 | −13.3 | −25.6 | 0.8 |
| 2–79 | ZKA135-39 | 177.1 | −8.9 | −12.3 | −19.8 | 1836.1 |
| 2–80 | ZKA135-39 | 179.1 | −9.2 | −13.6 | – | 617.7 |
| 2–77 | ZKA143-35-1 | 183 | −10.0 | −13.4 | – | 445.0 |
| 2–78 | ZKA143-35-1 | 185.1 | −9.9 | −13.3 | – | 37.3 |
| 147 | ZKA147-39 | 180 | −9.7 | −12.5 | −17.7 | 3480.2 |
| | ZK159-47-04 | 171.4 | – | – | 9.9 | 2.2 |
| 22 | ZKA183-87 | 121.43 | – | – | −33.4 | 2.6 |
| | ZKA271-71a | 184.7 | – | – | 7.2 | 2.0 |
| 2–45 | ZKB71-12 | 287.6 | −16.9 | −11.5 | – | 191.0 |
| 2–47 | ZKB71-12 | 293.9 | −16.4 | −13.7 | – | 193.1 |
| 2–60 | ZKB87-32 | 297.9 | −17.1 | −13.0 | – | 48.0 |
| 2–62 | ZKB87-32 | 303 | −17.2 | −11.7 | −11.2 | 290.1 |

–: No measurement.

and specimen holders, and has a guaranteed spatial resolution of 0.1 nm (crystal lattice) or 0.18 nm (point to point), and the smallest probe size of 0.8 nm.

Fourteen samples were analyzed for carbon and oxygen isotopic composition of the calcite cement in the sandstone samples (Table 1). The samples were ground to >200 mesh and then combusted at 300 °C under vacuum for half an hour to remove organic matter. Subsequently, the samples were digested with 100% phosphoric acid and analyzed for their respective carbon and oxygen isotopic composition.

### 3.2. Organic geochemistry

Abundant fluid inclusions were observed within calcite cements and within quartz that fills fractures in the sandstone under a UV microscope. Some oil also occurs in adsorbed form onto sandstone framework minerals (quartz, feldspar, rock fragments). A subset of the sandstone samples (4 samples, Table 2) was selected for analysis of organic compounds in oil. The two forms of oil (in fluid inclusions and adsorbed onto minerals) were extracted and analyzed using a method similar to that reported by George et al. (2004). The first step involved extraction of the adsorbed oil from mineral surfaces. The sample cuttings were disaggregated, crushed to ~60 mesh in dichloromethane ($CH_2Cl_2$) to release the

Table 2
Organic geochemical parameters for fluid inclusion oils and adsorbed oils from Zhiluo Formation sandstones

| Type | No. | *n*-Alk max | Pr/Ph | Pr/*n*C$_{17}$ | Ph/*n*C$_{18}$ | OEP | Ts/Tm | DTs/DTm | $C_{23}$ TT/30H | $C_{19}$TT/($C_{19}$+$C_{23}$)TT | $C_{26}$/$C_{25}$ TT | $C_{24}$Te/($C_{24}$Te+$C_{23}$TT) | $C_{30}$ hopanes αβ/(αβ+βα) | D29/30H | D29/29H | Gamm/30H | $C_{32}$ hopanes 22S/(22S+22R) | $C_{27-29}$ steranes/$C_{29-33}$ 17α hopanes | $C_{29}$ ααα 20S/(20S+20R) | $C_{27}$% ααα | $C_{28}$% ααα | $C_{29}$% ααα | MPI |
|---|---|---|---|---|---|---|---|---|---|---|---|---|---|---|---|---|---|---|---|---|---|---|---|
| Fluid inclusion oils | 147 | $C_{25}$ | 0.33 | 3.57 | 2.36 | 1.04 | 1.47 | tr | 0.51 | 0.06 | 1.19 | 0.29 | 0.90 | 0.13 | 0.22 | 0.17 | 0.57 | 0.56 | 0.56 | 41 | 25 | 34 | 0.49 |
| | 2–47 | $C_{23}$ | 0.21 | 0.53 | 0.57 | 1.04 | 1.06 | 1.03 | 0.30 | tr | 1.34 | 0.30 | 0.90 | 0.18 | 0.26 | 0.20 | 0.61 | 0.84 | 0.49 | 35 | 28 | 37 | 0.50 |
| | 2–62 | $C_{22}$ | 0.27 | 0.53 | 0.85 | 1.06 | 1.13 | 1.16 | 0.32 | 0.02 | 1.47 | 0.29 | 0.91 | 0.17 | 0.26 | 0.16 | 0.62 | 0.95 | 0.51 | 43 | 25 | 32 | 0.79 |
| | 2–78 | $C_{22}$ | 0.57 | 0.41 | 0.58 | 1.00 | 1.10 | 1.11 | 0.32 | 0.04 | 1.38 | 0.29 | 0.89 | 0.17 | 0.25 | 0.17 | 0.62 | 0.86 | 0.52 | 39 | 27 | 35 | 0.40 |
| Adsorbed oils | 2–47 | $C_{23}$ | 0.71 | 0.54 | 0.73 | 1.09 | 1.00 | 0.97 | 0.16 | 0.07 | 1.43 | 0.28 | 0.89 | 0.28 | 0.52 | 0.17 | 0.60 | 0.60 | 0.56 | 44 | 27 | 29 | 0.36 |
| | 2–62 | $C_{23}$ | 0.40 | 0.66 | 0.68 | 0.94 | 1.12 | 1.22 | 0.32 | 0.03 | 1.44 | 0.30 | 0.90 | 0.18 | 0.29 | 0.17 | 0.61 | 0.78 | 0.53 | 39 | 27 | 34 | 0.54 |
| Oil sandst | T-oil | $C_{20}$ | 0.87 | 0.28 | 0.30 | 1.04 | 5.02 | tr | 1.54 | 0.38 | 1.35 | 0.18 | 0.93 | tr | tr | 0.04 | 0.66 | 0.93 | 0.56 | 29 | 28 | 43 | 0.79 |
| Sour. rock | T-source | $C_{21}$ | 0.80 | 0.25 | 0.25 | 1.07 | 4.56 | tr | 0.27 | 0.17 | 1.66 | 0.28 | 0.93 | tr | tr | 0.14 | 0.59 | 0.68 | 0.62 | 29 | 27 | 44 | – |

Note: OEP: $(C_{25}+6*C_{27}+C_{29})/(4*C_{26}+4*C_{28})$; TT: tricyclic terpane; Te: tetracyclic terpane; Gamm: Gammacerane; ααα denotes 5(H), 14(H), 17(H) steranes; MPI = methylphenanthrene index (1.5*[3-MP+2-MP]/[P+9-MP+1-MPI]); for other peak abbreviations see Fig. 8; –: no measurement.

adsorbed oil into the solvent, and the oil was collected. The second step involved extraction of oil from fluid inclusions. After calcite was dissolved in HCl, quartz grains were first separated from other minerals, and then potential contamination was removed using successive treatments of $H_2O_2$ and $CH_2Cl_2$. The quartz grains were subsequently crushed to ~200 mesh in $CH_2Cl_2$ to release oil from the inclusions in quartz grains.

For comparison, an oil-rich sandstone (T-oil) and a potential source rock (T-source) (TOC = 1.1%) of the Triassic from the nearby Ansai oilfield (Fig. 1) were also analyzed along with the host sandstone. T-oil and T-source were extracted and separated into saturated, aromatic, resin and asphaltene fractions by column chromatography using *n*-pentane, $CH_2Cl_2$, and methanol as developing solvents.

Because of the small quantity of oil released from the sandstone samples (Table 1), whole oil samples were directly analyzed. For the T-oil, the saturated and aromatic fractions were analyzed separately. For the T-source, only the saturated fraction was analyzed. All these analyses were performed with a Hewlett Packard 6890GC/5973MSD-mass spectrometer. The gas chromatography (GC) was fitted with a HP-5MS capillary column (30 m × 0.25 mm × 0.25 μm). The temperature of sample injection was 300 °C and the oven was held at 50 °C for 1 min. The temperature was then increased from 50 °C to 310 °C at a rate of 3 °C/min, and then held at 310 °C for 18 min. Helium was used as a carrier gas (1.0 mL/min). Operating conditions were: ion source, 230 °C; emission current, 34.6 μA; quadruple temperature, 150 °C and electron energy, 70 eV.

## 4. Results

### 4.1. Mineralogical and stable isotope data

Microbe-like structures were found in those sandstone samples with high U content, such as in those from wells

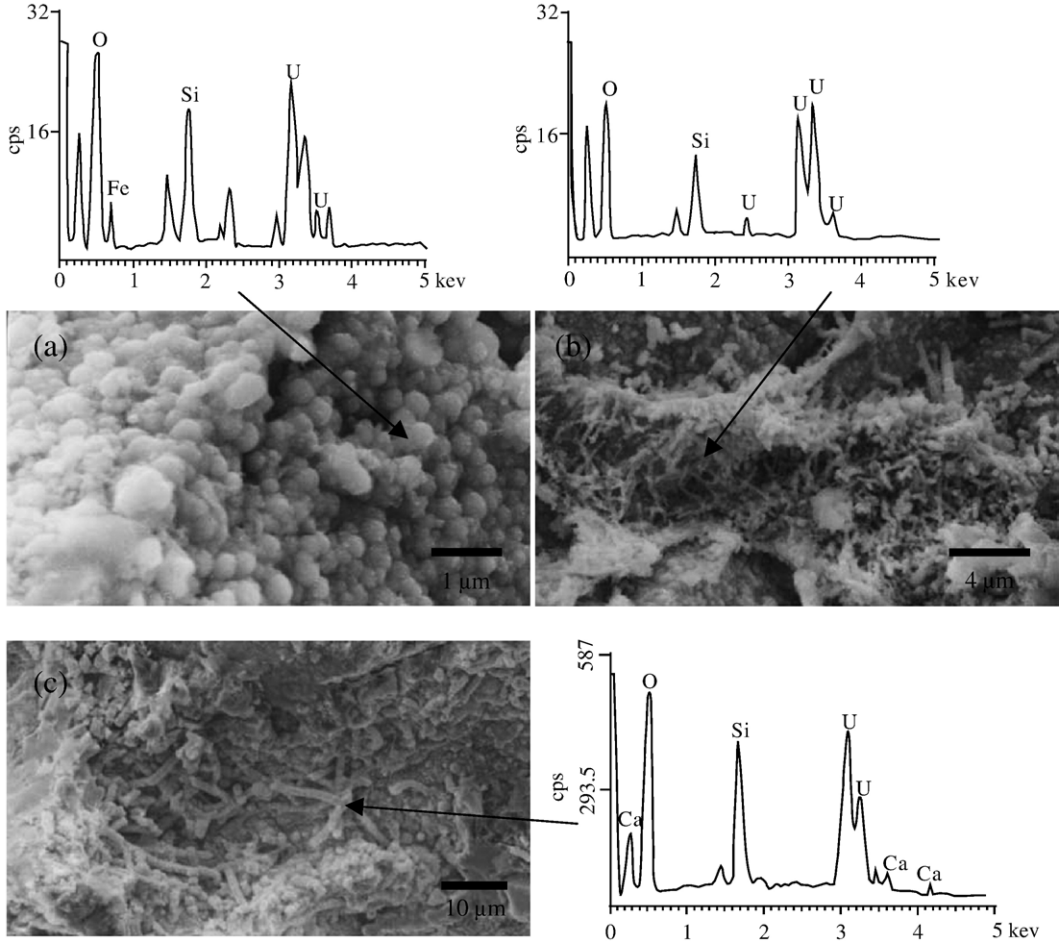


Fig. 3. SEM photographs showing coccoid (a) and rod-shaped (b and c) structures in a sandstone from well ZKA147-39 (depth = 180 m) with U, Si and Ca (likely coffinite) present as major elements (EDS data). The samples were carbon coated.

ZKA135-39 and ZKA147-39 with a uranium content of 1836 μg/g and 3480 μg/g, respectively (Table 1). The structures occur within pyrite aggregates and have lengths from 0.3 to 12 μm and widths from 0.1 to 2 μm. They occur as globular cocci (Fig. 3a) and long rods (Fig. 3b and c). The rod-shaped structures have similar morphology as those of *Desulfobacterium vacuolatum* and *Desulfovibrio piger* (Widdel and Bak, 1999), although positive identification of these structures is beyond the scope of this study. EDS analyses show that the microorganism-like structures have 39 to 64.5 wt.% U, 8.7 to 13.4 wt.% Si, and trace to 2.8 wt.% Ca (Fig. 3), sometimes with a small amount of Al, Fe, Mg, S, P and V. The chemical composition of the structures is typical for Ca-bearing coffinite or pure coffinite [$(USiO_4)_{1-x}(OH)_{4x}$]. Coffinite may have pseudomorphically replaced microbes. High-resolution TEM lattice-fringe images of the coffinite in Fig. 3c show the existence of coffinite nanoparticles ranging in size from 4 nm (Fig. 4a) to 80 nm (Fig. 4b), mostly from 5 to 25 nm (Fig. 5). Fourier transform images and crystallographic analysis of the selected-areas in Fig. 4a and b show that the nanoparticles have d-spacings of 3.44 Å to 3.48 Å (lower left insets of Fig. 4a and b), 4.66 Å (Fig. 4b upper left inset) and 2.64 Å (not shown), confirming the nanoparticles as coffinite (tetragonal dipyamid) with a composition of U, Si, Ca, Al, K, C and P (Fig. 4c). The elements Ca, K, C and P may be derived from incorporation of inorganic ions during coffinite crystallization. However, the presence of certain elements, such as P, C and K, could be indicators of ancient biological activity.

SEM observation shows that the coffinite is intimately intergrown or juxtaposed with secondary pyrite; calcite cement is frequently observed to co-exist with pyrite (Fig. 6). The co-existence of secondary pyrite, calcite and coffinite and the lack of any replacement texture suggest simultaneous precipitation of these minerals or a genetic link between them. The pyrite occurs mainly as aggregates. The $\delta^{34}S$ values of the pyrite aggregates range from −39.2‰ to +15.8‰ ($n=12$). The $\delta^{13}C$ values of calcite range from −1.4‰ to −17.2‰ ($n=14$) (Table 1). The $\delta^{13}C$ values of calcite have been reported to be as negative as −33‰ (Wang et al., 2005) in the host sandstone in the area.

### 4.2. Organic geochemistry

The oil inclusions within calcite and quartz have similar light blue to bright white fluorescence emission colors, suggesting that the oil inclusions from different host minerals (calcite and quartz) have similar compositions, although George et al. (2001) suggested that the

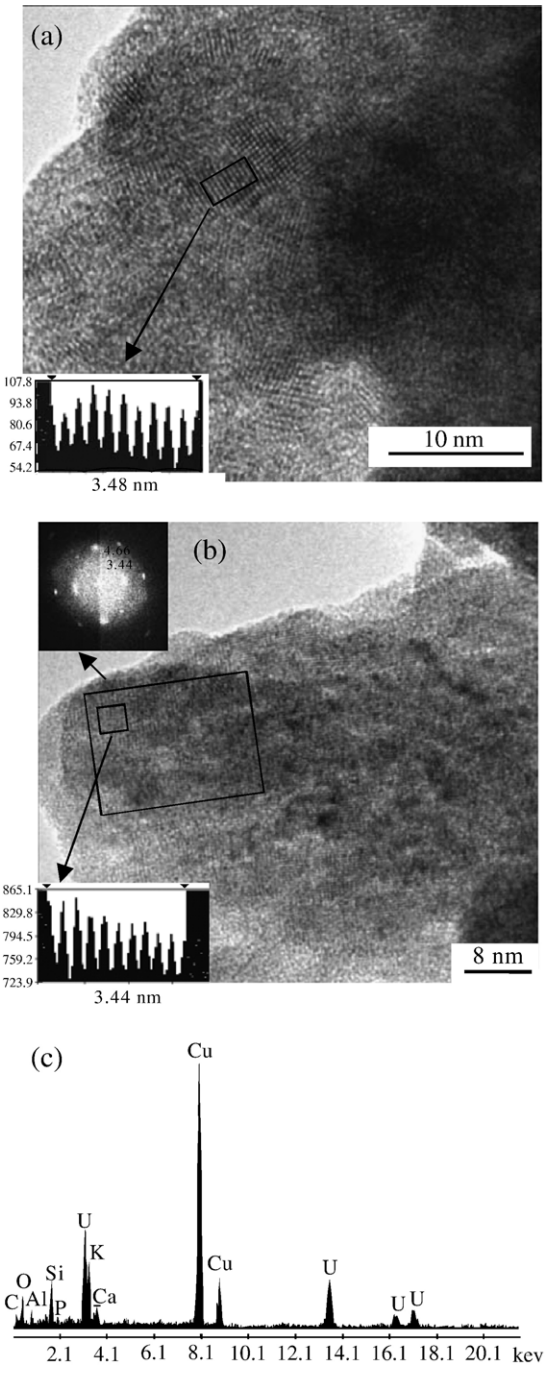


Fig. 4. (a) and (b): TEM lattice fringe images from a small area in Fig. 3c showing nanoparticles of coffinite with d-spacing measurements (lower-left insets) and Fourier transform image (upper-left inset of Fig. 2b); (c) An EDS composition of the same area shows the presence of U, Si, Ca, Al, K, C and P. The sample was recovered from a SEM carbon-disc, broken into small pieces and mounted onto a TEM Cu grid. No carbon coating was performed.

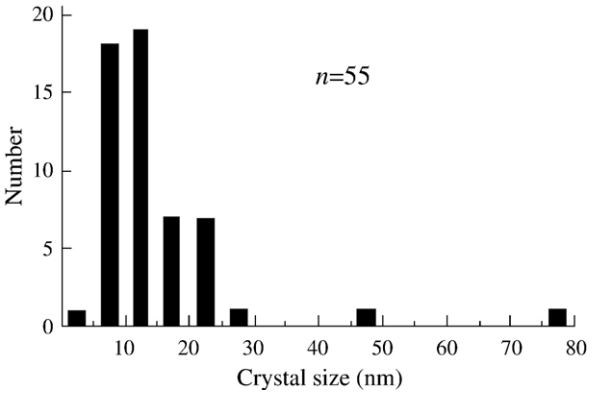


Fig. 5. Histogram showing the majority of crystals in the microorganism-like structures in Fig. 3c have sizes ranging from 5 to 25 nm.

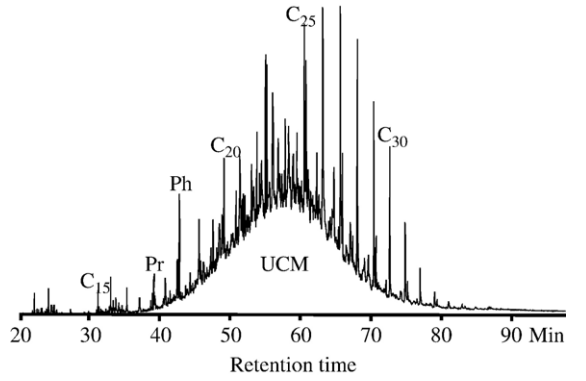


Fig. 7. Mass chromatogram (*m*/*z* 85) showing a hump of unresolved complex mixtures (UCM) in oil-bearing fluid inclusions extracted from the well ZKA147-39 sandstone (depth = 180 m). Pr: Pristane; Ph: Phytane.

maturity of an oil inclusion is not necessarily related to visually-determined fluorescence colors.

GC-MS data (*m*/*z* = 85) for four fluid inclusion (FI) oils and two adsorbed oils (Table 2) show that Pr/$nC_{17}$ and Ph/$nC_{18}$ ratios range from 0.41 to 3.6 and 0.58 to 2.36, respectively, significantly higher than those of the T-oil and T-source samples (0.25 to 0.28 and 0.25 to 0.30, respectively). The ratios are also much higher than those for oils produced from the Ansai oilfield in the Ordos basin (0.24 to 0.36; Guo et al., 2006). The FI oils and adsorbed oils show prominent baseline humps of unresolved complex mixtures (UCM), for example, in the $C_{16}$ to $C_{30}$ carbon number range centering at about $C_{23}$ (Fig. 7). The two types of oils contain $C_{26}$ to $C_{32}$ 17α, 21β 25-norhopanes and demethylated $C_{28}$ to $C_{29}$ tricyclic terpanes (Fig. 8a, b). $C_{29}$ 17α, 21β 25-norhopane (29DH) is relatively abundant with the 29DH/30H (30H = $C_{30}$ 17α, 21β hopane) ratio ranging from 0.13 to 0.28, and 29DH/29H (29H = $C_{29}$ 17α, 21β 30-norhopane) from 0.22 to 0.52 (Table 2). In contrast, no significant 25-norhopanes were detected in the T-oil and

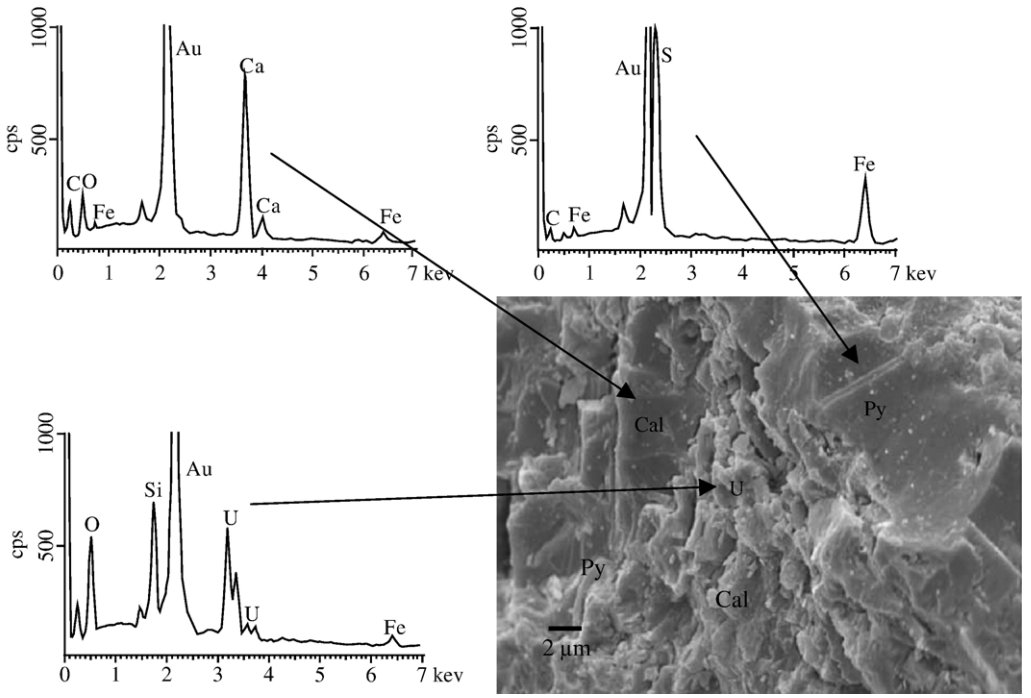


Fig. 6. SEM photograph showing the co-existence of secondary pyrite, calcite and coffinite from the well ZKA135-39 sandstone, identified using EDS. The samples were Au-coated.

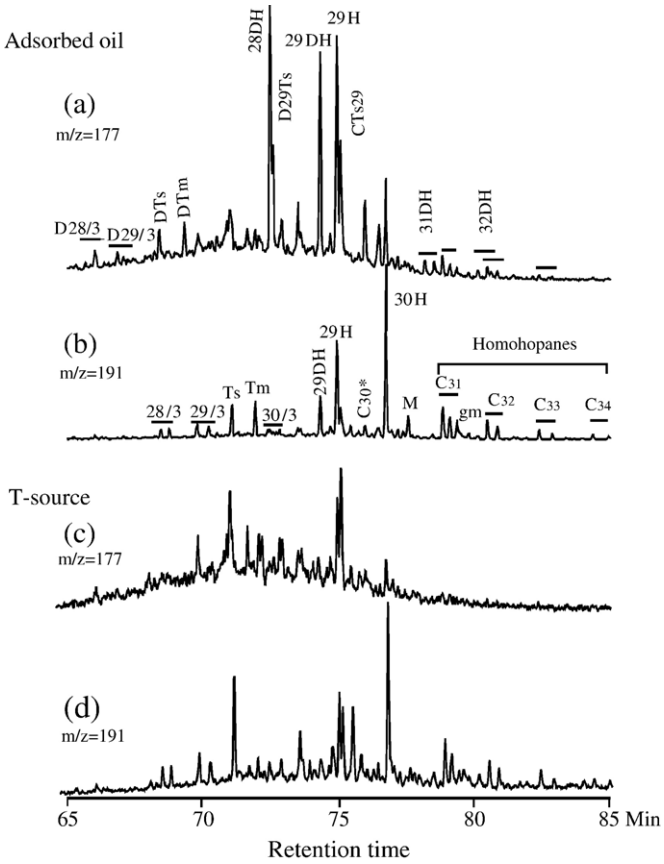


Fig. 8. Partial *m/z* 191 and 177 mass chromatograms showing existence of abundant demethylated hopanes and tricyclic terpanes in an adsorbed oil extracted from sandstone in well ZKB71-12 (depth=293.9 m) (a, b); No significant amounts of these compounds are present in a potential source rock in the Triassic (c, d). Compounds identifications: H: 17α, 21β hopanes; M: $C_{30}$ 17β, 21α moretane; D: 25-norhopanes; $C_{30}^{*}$: $C_{30}$ 17α, 21β diahopane; 29Ts: $C_{29}$ 18α, 21β 30-norhopane; gm: gammacerane; 28/3: $C_{28}$ tricyclic terpane; 29/3: $C_{29}$ tricyclic terpane; D28/3: $C_{27}$ demethylated tricyclic terpane; Ts: 18α, 21β-22, 29, 30-trisnorhopane; DTs: $C_{26}$ 18α, 21β-22, 25, 29, 30-tetrakisnorhopane (or 25-nor Ts); Tm: 17α, 21β-22, 29, 30-trisnorhopane; DTm: 25-nor Tm; etc.

T-source (Fig. 8c, d; Table 2) or in the oils from the Ansai oilfield (Guo et al., 2006).

Maturity-related parameters including OEP (Odd Even Predominance index), $C_{30}$ hopane αβ/(αβ+βα), $C_{32}$ homohopane 22S/(22S+22R), $C_{29}$ sterane 20S/(20S+20R) ratios for all the analyzed samples show similar values (Table 2). The OEP index ranges from 0.94 to 1.07, $C_{30}$ hopane αβ/αβ+βα from 0.89 to 0.93, $C_{32}$ 22S/(S+R) from 0.57 to 0.62, and $C_{29}$ sterane 20S/(S+R) from 0.49 to 0.62. The values are close to the respective equilibrium values (Peters and Moldowan, 1993), suggesting that organic matter from all the analyzed samples has reached an early to peak oil window. The methylphenanthrene index (Radke and Welte, 1983) for the FI oils and adsorbed oils ranges from 0.36 to 0.79 with a calculated vitrinite reflectance ($R_o$) value of 0.61% to 0.88%. The values are close to the $R_o$ value of 0.75% for the Triassic source rock of the Ansai oilfield (Guo et al., 2006) and the $R_o$ value of 0.62% to 1.07% for the Triassic rocks in the whole Ordos basin (Chen and Huang, 1997), but significantly higher than those of the Jurassic (0.36% to 0.49%) (Ren et al., 2006) and lower than those of the Carboniferous–Permian rocks (1.4% to 2.0%) (Cai et al., 2005a).

All the analyzed samples show similar values in biological precursor-related parameters except for abnormally high tricyclic terpanes for T-oil. All the analyzed samples in Table 2 show that the $C_{23}$ tricyclic terpane is the most abundant, with a low $C_{19}/(C_{19}+C_{23})$ tricyclic terpane ratio ranging from trace to 0.17. The $C_{24}$ tetracyclic terpane is present in lesser amounts than the $C_{23}$ tricyclic terpane (Table 2). The relatively low $C_{19}/(C_{19}+C_{23})$ tricyclic terpane and $C_{24}$ tetracyclic terpane/($C_{24}$ tetracyclic terpane+$C_{23}$ tricyclic terpane) ratios indicate a low terrestrial organic matter input to these oils (e.g. Preston and Edwards, 2000). The $C_{26}$ tricyclic terpanes are more abundant than the $C_{25}$ tricyclic

terpanes with $C_{26}/C_{25}$ triterpane ratio ranging from 1.34 to 1.67, a characteristic that is diagnostic for sourcing from a lacustrine facies (Schiefelbein et al., 1999). Lacustrine algae mixed with terrestrial plants as precursors of the oils are supported by the relative abundance of ααα steranes ($C_{27}>C_{28}<C_{29}$), moderate ratios of $C_{27}$ to $C_{29}$ regular steranes/$C_{29}$ to $C_{33}$ 17α hopanes and small amounts of gammacerane detected in all the samples (Table 2).

Thus, all the above features indicate that the FI oils and adsorbed oils are well correlated with the T-source, suggesting that the oils were most likely derived from the Triassic source rock with the $R_o$ values ranging from 0.6 to 0.9% and lacustrine algae and terrestrial higher plants as organic precursors.

## 5. Discussion

The sandstone that hosts abundant microorganism-like structures and coffinite is shown to have an average pyrite $\delta^{34}S$ value of −17.7‰, an average calcite $\delta^{13}C$ of −9.7‰, a U content of 3480 μg/g. The sandstone also contains oil trapped in fluid inclusions that has a large UCM and 25-norhopanes, consistent with biodegradation prior to trapping (Volkman et al., 1983). These features, along with the co-existence of the mineral assemblage coffinite, pyrite, and calcite, suggest an intimate association between microorganism-like structures, uranium reduction, sulfate reduction, and oil biodegradation.

### 5.1. Biogenic origin of pyrite and petroleum-derived carbon of calcite

The wide range of $\delta^{34}S$ values in pyrite (Table 1) and the lightest value of −39‰ indicate that pyrite is biogenic and was formed by bacterial sulfate reduction (e.g. Machel et al., 1995; Cai et al., 2002, 2005b). This conclusion is strengthened by the fact that the host sandstone was never heated above 70 °C (Ren et al., 2006), as indicated by a vitrinite reflectance value from 0.36% to 0.49% ($n=7$) and burial and geothermal history of Well S1, which is close to the Shashagetai deposit (Fig. 1). Microbes are generally active at low temperatures (<80 °C) (Wilhelms et al., 2000) although sulfate-reducing archaea have been found at temperatures up to 110 °C (e.g. Stetter et al., 1993).

The co-existing calcite cements have $\delta^{13}C$ values as negative as −17‰ reported in this study (Table 1) and −33‰ reported by Wang et al. (2005). The low molecular weight components of petroleum are isotopically lighter, and lighter compounds are the ones most soluble in water where biodegradation takes place. These components are thus likely to be utilized preferentially by microbes, resulting in isotopically lighter $CO_2$ during the earlier stage of petroleum (likely methane) biodegradation. As biodegradation proceeds, heavier hydrocarbons are degraded to generate isotopically heavier $CO_2$, thus explaining the wide range of the calcite $\delta^{13}C$ values, mainly ranging from −10‰ to −33‰. However, the calcite carbon may have been derived from mixing of inorganically-derived $CO_2$ with petroleum-derived $CO_2$ (e.g. Machel et al., 1995), although coal and kerogen cannot be ruled out as possible sources. Co-precipitation of biogenic pyrite aggregates and petroleum-derived calcite suggests bacterial sulfate reduction was coupled with anaerobic oxidation of petroleum hydrocarbons.

### 5.2. Anaerobic oxidation of petroleum hydrocarbons

The FI oils and adsorbed oils in the Shashagetai deposit were most likely derived from the Triassic lacustrine mudstone as the oils show values of maturity-related and organic precursor-related parameters that are similar to the Triassic source rock and its derived oil. In contrast, the oils show significant differences to oil derived from humic kerogen from the Jurassic and the Carboniferous–Permian rock strata.

The oils contain abundant *n*-alkanes and significant amounts of 25-norhopanes and demethylated tricyclic terpanes (Figs. 7 and 8a, b). The presence of 25-norhopanes in crude oil is commonly recognized as an indicator of severe biodegradation. 25-Norhopanes in the oil are commonly generated by bacterial removal of the methyl group at C-10 from the regular hopanes (Volkman et al., 1983). However, because 25-norhopanes have been detected as free hydrocarbons in certain petroleum source rocks (e.g., Noble et al., 1985; Blanc and Connan, 1992), they could have been derived from source rocks and concentrated in host rocks, due to their resistance to subsequent biodegradation. Thus, oil inclusions with 25-norhopanes and abundant *n*-alkanes could have been derived from the source rock in the Ordos Basin and may not necessarily be an indicator for biodegradation. However, this scenario is not the case for the U-containing host sandstones in this study, because no significant 25-norhopanes and demethylated tricyclic terpanes were detected in the source rock and its derived oil.

25-Norhopanes as biodegradation products have been shown by previous studies. For example, Volkman et al. (1983) and Bennett et al. (2006) have demonstrated biological transformation of hopanes to 25-norhopanes. Thus, a biodegraded oil is expected to have an increased 29DH/30H and 29DH/29H. The high ratios for the oils in the host sandstone in this study (Table 2) likely result

from heavy biodegradation, which is supported by the occurrence of a UCM in the oils, although it is difficult to evaluate whether a UCM may have been generated by uranium radiation damage. However, Turner et al. (1993) have argued against chemical and isotopic variation as a result of radiation damage for organic matter in the Grants uranium region, New Mexico as proposed by Leventhal (1980). Because the general sequence of biodegradation of biomarkers is *n*-alkanes followed by isoprenoids, steranes, hopanes/diasteranes, and aromatic steroids, abundant alkanes in the studied oils may have been a result of a later input of fresh oil, after biodegradation. The later oil was slightly biodegraded as indicated by significantly higher Pr/$nC_{17}$ and Ph/$nC_{18}$ ratios than those of the possible source rock and its derived oil, respectively (Table 2). Thus, the FI oils and adsorbed oils may represent a mixture of a later, slightly biodegraded oil and an early, heavily biodegraded oil (Volkman et al., 1983).

It is not clear if the biodegradation of the oils is an oxic or anoxic process. However, an increasing number of novel microorganisms have recently been shown to utilize methane and saturated and aromatic hydrocarbons as growth substrates in syntrophic cocultures with other anaerobes under strictly anoxic conditions (e.g. Aeckersberg et al., 1991; Boetius et al., 2000; Zhang et al., 2002). Sulfate-reducing bacterial strain Hxd3 (related to the genus *Desulfococcus*), strain TD3, and strain Ak-01 have been reported to be capable of growing anaerobically on $C_{12}$ to $C_{20}$, $C_6$ to $C_{16}$ and $C_{13}$ to $C_{18}$ alkanes, respectively, to completely oxidize them to carbon dioxide (Aeckersberg et al., 1991; Rueter et al., 1994; So and Young, 1999; So et al., 2003) with fatty acids as intermediate products:

$$SO_4^{2-} + 1.33(-CH_2) + 0.66H_2O \Rightarrow H_2S\uparrow + 1.33CO_2\uparrow + 2OH^-$$

Anaerobic degradation of petroleum hydrocarbons has recently been shown to have a similar sequence of removal of saturated hydrocarbon types (e.g. Hunkeler et al., 1998; Head et al., 2003). Thus, the FI oils and adsorbed oils in coexistence with biogenic sulfides are most likely to have been degraded by anaerobic microorganisms (e.g. Cai et al., 2002, 2005b).

Because the host sandstones were never heated over 70 °C, the environment was favorable for microbial activity. Thus, early biodegradation of the oils may have taken place soon after oil emplacement into the host sandstones. The oil emplacement is expected to have occurred simultaneously with a peak oil generation of the Triassic mudstone, i.e., during the end of the Early Cretaceous to the Late Cretaceous. Later charged oil was likely derived from the leakage of ancient oil pools due to subsequent movements, perhaps during the Neogene Himalayan Orogeny. The reasons are several folds. First, no significant petroleum has been generated since the Late Cretaceous in the basin. Second, the later charged oil is shown to have similar maturity to the earlier oil as indicated by similar values of the Ts/Tm and DTs/DTm ratios (Table 2). The DTs/DTm ratio has been considered to be an efficient parameter to indicate maturity of an early heavily degraded oil (Volkman et al., 1983). Third, the later charged oil is well correlated with the Triassic source rock. Fourth, petroleum has been shown to distribute along the fault F1 (Fig. 1) (Zhang et al., 2006). All these features along with the evidence that later charged oil was slightly degraded indicate that biodegradation of the oils may have been prior to trapping in quartz grains and calcite cements. That is, biodegradation of the oils may have taken place during the period from the end of the Early Cretaceous to the Neogene.

### 5.3. Uranium bio-reduction and mineralization

The mineralized structures found in the study contain mineralogical biosignatures including morphology and size, and thus are interpreted to be fossilized microbes (Milodowski et al., 1990; Watterson, 1991; Min et al., 2005; Reith et al., 2006). This proposal is supported by the fact that the coffinite that pseudomorphically replaced microbes shows nano-crystals with size ranging mainly from 5 to 25 nm. Nanometer-size uraninite ($UO_2$) has been shown to be the products of uranium bioreduction (Lovley and Philips, 1992; Suzuki et al., 2002), and most biominerals generated by microorganisms are nanoparticles (Banfield and Zhang, 2001). Other lines of evidence for the biogenic origin of coffinite in the study are summarized as follow: 1) The coffinite in the structures contain elements characteristic of ancient biological activity such as P and K; 2) The coffinite is intimately intergrown with biogenic pyrite and calcite of petroleum-derived carbon; 3) The host sandstone with the structures are shown to have fluid inclusion oils and adsorbed oils degraded by microorganisms. Thus, the structures are inferred to be a result of microbial in the Shashagetai uranium deposit.

The roles of microorganisms in uranium biomineralization include U(VI) biosorption and reduction of U(VI) to U(IV) (e.g. Gadd, 1996). Fe(III)-reducing bacteria such as *Geobacter metallireducens* and *Shewanella putrefaciens* and sulfate-reducing bacteria such as *Desulfovibrio* Species (*D. desulfuricans*, *D. vulgaris*, and *D. baculatum*), *Desulfotomaculum reducens*, *Desulfuromonas acetoxidans* and *Desulfosporosinus* spp. have been shown experimentally

to be capable of reducing U(VI) to V(IV) (Lovley et al., 1991, 1993; Lovley and Philips, 1992; Suzuki et al., 2002). However, uranium reduction by *D. desulfuricans* is inhibited between 17 mM and 24 mM $U^{6+}$ due to the toxicity and radioactivity of uranium (Lovley and Philips, 1992). Thus, Min et al. (2005) have suggested that accumulation of U, after bacterial growth had stopped, was likely responsible for the formation of the biogenic coffinite in the roll-front deposits in the Yili and Tuha basins in NW China. The accumulation of U is generally considered to occur between uranium species and negatively charged sites on non-living microorganisms (Suzuki and Banfield, 1999), so no change of U valence is expected. However, in the sandstone-hosted U deposits in the Shashagetai and other areas, U is mainly present as tetravalent coffinite and uraninite, and no hexavalent U mineral has been reported to coat uraninite or coffinite. This observation suggests that the uptake of U by non-living microbes may not be as important as previously thought. The concurrent precipitation of pyrite and coffinite in the Shashagetai deposit suggests that U(VI) was reduced by microbes in an environment where sulfate reduction was the predominant terminal electron-accepting process. Some investigations have shown that living organisms isolated from uranium mines show especially high ability to accumulate uranium (Panak et al., 1998; Sakaguchi, 1998). These results suggest that microorganisms can develop resistance to toxic metals in the environment by genetic and/or physiological adaptation (Gadd, 1990). For example, some microbes may have utilized precipitation of toxic metal complexes as a biological detoxification mechanism (Reith et al., 2006). Thus, it is possible that some microbes are able to live under a high U environment leading to the formation of U deposit in the Shashagetai region.

The occurrence of the microbe-like structures in association with biodegraded hydrocarbons, coffinite and calcite with petroleum-derived carbon may suggest that anaerobic oxidization of petroleum is coupled with reduction of sulfate and U(VI), although it is unknown if this U(VI) reduction is a result of activity of a single species or a consortia of different microbes. The microbial species responsible for this process are yet to be identified.

### 5.4. Implications

The petroleum deposit in the Ordos Basin provides abundant organic carbon for uranium biomineralization by bacteria. The natural association between petroleum and uranium ore may be used as a guide to explore these deposits. For example, if a uranium ore deposit is associated with petroleum in shallow rock strata, petroleum pools are likely to be present in deep strata. In the case of the Shashagetai deposit, commercial oil/gas deposits have been discovered in the area close to the uranium ore deposit. Hydrocarbon seepage is detected in the surface soil and it has been attributed to fault F1 as a conduit for petroleum to flow upward (Fig. 1) (Zhang et al., 2006 and references therein). Thus, it is possible to explore for deep oil/gas pools through the detection of soil gas hydrocarbon or/and radiation anomalies in shallow strata.

## 6. Conclusions

Microbe-like structures found in the uranium deposit from the Ordos Basin, NW China are composed of nanoparticles of coffinite with size ranging from 5 to 25 nm. These structures contain biosignatures including morphology, size, and bio-elements such as P and K. Oil inclusions and adsorbed oils are found to co-exist with the microbe-like structures in the host sandstones, and are shown to have been derived from Triassic lacustrine algae mixed with terrestrial organic matter. The oils show abundant *n*-alkanes, 25-norhopanes and demethylated tricyclic terpanes and the occurrence of unresolved complex mixtures. These features are thus interpreted to be mixtures of a later charged oil and an early heavily biodegraded oil. Subsequently, the oils were slightly biodegraded, resulting in increased Pr/$nC_{17}$ and Ph/$nC_{18}$ ratios. Anaerobic biodegradation of petroleum may have been coupled with bio-reduction of sulfate and U(VI), thus explaining the natural association of the microorganism-like structures, coffinite, biodegraded petroleum and biogenic pyrite aggregates in the uranium-containing sandstone in the Ordos Basin, NW China.

## Acknowledgements

The research was financially supported by China National Major Basic Development Program “973” (2003CB214605), National Natural Sciences Foundation of China (40573034) and FANEDD to CC. We are grateful to Dr. Simon George and an anonymous reviewer for their critical comments, which helped to improve the MS. This research was also supported by a NSF grant (EAR-0345307) to HD and a NSF of China (40472064) to HD.

## References

Abdelouas, A., Lu, Y., Lutze, W., Nuttall, H.E., 1998. Reduction of U (IV) to U(IV) by indigenous bacteria in contaminated ground water. Journal of Contaminant Hydrology 35, 217–233.

Aeckersberg, F., Bak, F., Widdel, F., 1991. Anareobic oxidation of saturated hydrocarbons to $CO_2$ by a new type of sulfate-reducing bacterium. Archives of Microbiology 156, 5–14.

Banfield, J.F., Zhang, H.Z., 2001. Nanoparticles in the environment. In: Banfield, J.F., Navrotsky, A. (Eds.), Nanoparticles and the Environment. Reviews in Mineralogy and Geochemistry, vol. 38, pp. 393–432.

Bennett, B., Fustic, M., Farrimond, P., Huang, H.P., Larter, S.L., 2006. 25-Norhopanes: formation during biodegradation of petroleum in the subsurface. Organic Geochemistry 37, 787–797.

Blanc, Ph., Connan, J., 1992. Origin and occurrence of 25-norhopanes: a statistical study. Organic Geochemistry 18, 813–828.

Boetius, A., Ravenschlag, K., Schubert, C.J., Rickert, D., Widdel, F., Gleseke, A., Amann, R., Jorgensen, B.B., Witte, U., Pfannkuche, O., 2000. A marine microbial consortium apparently mediating anaerobic oxidation of methane. Nature 407, 623–626.

Cai, C.F., Hu, G.Y., He, H., Li, J., Li, J.F., Wu, Y.S., 2005a. Geochemical characteristics and origin of natural gas and thermochemical sulfate reduction in Ordovician carbonates in the Ordos Basin, China. Journal of Petroleum Science and Engineering 48, 209–226.

Cai, C.F., Worden, R.H., Wang, Q.H., Xiang, T.S., Zhu, J.Q., Chu, X.L., 2002. Chemical and isotopic evidence for secondary alteration of natural gases in the Hetianhe Field, Bachu Uplift of the Tarim Basin. Organic Geochemistry 33, 1415–1427.

Cai, C.F., Worden, R.H., Wolff, G.A., Bottrell, S., Wang, D.L., Li, X., 2005b. Origin of sulfur rich oils and $H_2S$ in Tertiary lacustrine sections of the Jinxian Sag, Bohai Bay Basin, China. Applied Geochemistry 20, 1427–1444.

Chen, J.P., Huang, D.F., 1997. The source of oils in Jurassic coal mine in the southeast of Ordos basin. Acta Sedimentologica Sinica 15 (2), 100–104 (in Chinese).

Gadd, G.M., 1990. Metal tolerance. In: Edwards, C. (Ed.), Microbiology of Extreme Environments. Open University Press, Milton Keynes, pp. 59–88.

Gadd, G.M., 1996. Influence of microorganisms on the environmental fate of radionuclides. Endeavour 20, 150–156.

George, S.C., Ahmed, M., Liu, K., Volk, H., 2004. The analysis of oil trapped during secondary migration. Organic Geochemistry 35, 1489–1511.

George, S.C., Ruble, T.E., Dutkiewicz, A., Eadington, P.J., 2001. Assessing the maturity of oil trapped in fluid inclusions using molecular geochemistry data and visually-determined fluorescence colours. Applied Geochemistry 16, 451–473.

Guo, Y.Q., Li, W.H., Chen, Q.H., Cao, H.X., Zhang, D.F., 2006. Geochemical behaviors of oil and oil-source correlation in Yanchang-Yan'an Formations in Ansai-Fuxian area, Ordos basin. Oil and Gas Geology 27, 218–224.

Head, I.M., Jones, D.M., Larter, S.R., 2003. Biological activity in the deep subsurface and the origin of heavy oil. Nature 426, 344–353.

Hunkeler, D., Joerger, D., Haeberli, K., Hoehener, P., Zeyer, J., 1998. Petroleum hydrocarbon mineralization in anaerobic laboratory aquifer columns. Journal of Contaminant Hydrology 32, 41–61.

Leventhal, J.S., 1980. Organic geochemistry and uranium in the Grants Mineral Belt. In: Rautman, C.A. (Ed.), Geology and Mineral Technology of the Grants Uranium Region 1979. Memoir, vol. 38. New Mexico Bureau Mines and Mineral Resources, pp. 75–84.

Lovley, D.R., Philips, E.J.P., 1992. Reduction of uranium by *Desulfovibro desulfuricans*. Applied and Environmental Microbiology 58, 850–856.

Lovley, D.R., Philips, E.J.P., Gorby, Y.A., Landa, E.R., 1991. Microbial reduction of uranium. Nature 350, 413–416.

Lovley, D.R., Roden, E.E., Phillips, E.J.P., Woodward, P.J.C., 1993. Enzymatic iron and uranium reduction by sulfate-reducing bacteria. Marine Geology 113, 41–53.

Machel, H.G., Krouse, H.R., Sassen, R., 1995. Products and distinguishing criteria of bacterial and thermochemical sulfate reduction. Applied Geochemistry 10, 373–389.

Milodowski, A.E., West, J.M., Pearce, J.M., Hyslop, E.K., Basham, I.R., Hooker, P.J., 1990. Uranium-mineralized microorganisms associated with uraniferous hydrocarbons in southwest Scotland. Nature 347, 465–467.

Min, M.Z., Xu, M.H., Chen, J., Fayek, M., 2005. Evidence of uranium biomineralization in sandstone-hosted roll-front uranium deposits, northwestern China. Ore Geology Reviews 26, 198–206.

Nakashimima, S., Disnar, J.R., Perruchot, A., Trichet, J., 1984. Experimental study of mechanisms of fixation and reduction of uranium by sedimentary organic matter under diagenetic or hydrothermal conditions. Geochimica et Comochimica Acta 48, 2321–2329.

Noble, R., Alexander, R., Kagi, R.I., 1985. The occurrence of bisnorhopane, trisnorhopane and 25-norhopanes as free hydrocarbons in some Australian shales. Organic Geochemistry 8, 171–176.

Panak, P., Kutshke, S., Selenska-Pobell, S., Geipel, G., Bernhard, G., Nirsche, H., 1998. Bacteria from uranium mining waste pile: interaction with U(VI). Abstracts of Euro-conference on Bacteria–Metal/Radionuclide Interaction. Basic Research and Bioremediation 87–89.

Peters, K.E., Moldowan, J.M., 1993. The Biomarker Guide. Interpreting Molecular Fossils in Petroleum and Ancient Sediments. Prentice Hall, New Jersey.

Preston, J.C., Edwards, D.S., 2000. The petroleum geochemistry of oils and source rocks from the northern Bonaparte Basin, offshore northern Australia. The Australian Petroleum Production and Exploration Journal 40, 257–282.

Rackley, R.I., 1972. Environment of Wyoming Tertiary uranium deposits. American Association of Petroleum Geologists Bulletin 56, 755–774.

Radke, M., Welte, D.H., 1983. The methylphenanthrene index (MPI): a maturity parameter based on aromatic hydrocarbons. In: Bjorøy, M., et al. (Eds.), Advances in Organic Geochemistry. John Wiley, Chichester, pp. 504–512.

Reith, F., Rogers, S.L., McPhail, D.C., Webb, D., 2006. Biomineralization of gold: biofilms on bacterioform gold. Science 313, 233–236.

Ren, Z.L., Zhang, S., Gao, S.L., Cui, J.P., Liu, X.S., 2006. Relationship between thermal history and various energy mineral deposits in Dongsheng area, Yimen uplift. Oil and Gas Geology 27, 187–193.

Reynolds, R.L., Goldhaber, M.B., 1982. Biogenic and nonbiogenic ore-forming processes in the South Texas uranium district: evidence from the Panna Maria deposit. Economic Geology 77, 541–556.

Rueter, P., Rabus, R., Wilkes, H., Aeckersberg, F., Ralney, F.A., Jannasch, H.W., Wilddel, F., 1994. Anaerobic oxidation of hydrocarbons in crude oil by new types of sulphate-reducing bacteria. Nature 372, 455–457.

Sakaguchi, T., 1998. Removal and recovery of uranium by using microorganisms. Abstracts of Euro-conference on Bacteria–Metal/Radionuclide Interaction. Basic Research and Bioremediation, pp. 7–9.

Schiefelbein, C.F., Zumberge, J.E., Cameron, N.R., Brown, S.W., 1999. Petroleum systems in the South Atlantic margins. In: Cameron, N.R., Bate, R.H., Clure, V.S. (Eds.), The Oil and Gas Habitats of the South Atlantic. Geological Society of London Special Publication, pp. 169–179.

So, C.M., Young, L.Y., 1999. Isolation and characterization of a sulfate-reducing bacterium that anaerobically degrades alkanes. Applied and Environmental Microbiology 65, 2969–2976.

So, C.M., Phelps, C.D., Young, L.Y., 2003. Anaerobic transformation of alkanes to fatty acids by a sulfate-reducing bacterium, strain Hxd3. Applied and Environmental Microbiology 69, 3892–3900.

Stetter, K.O., Huber, R., Blöchl, E., Kurr, M., Eden, R.D., Fielder, M., Cash, H., Vance, I., 1993. Hyperthermophilic archaea are thriving in deep North Sea and Alaskan oil reservoirs. Nature 365, 743–745.

Suzuki, Y., Banfield, J., 1999. Geomicrobiology of uranium. In: Burns, P.C., Finch, R. (Eds.), Uranium: Mineralogy, Geochemistry and the Environment. Reviews in Mineralogy, vol. 38, pp. 393–432.

Suzuki, Y., Kelly, S.D., Kenneth, M.K., Banfield, J.F., 2002. Radionuclide contamination: nanometer-size products of uranium bioreduction. Nature 419, 134–136.

Turner, C.E., Fishman, N.S., Hatcher, P.G., Spike, E.C., 1993. Nature and role of organic matter in sandstone uranium deposits, Grants uranium region, New Mexico, USA. In: Parnell, J., Kucha, H., Landais, P. (Eds.), Bitumens in Ore Deposits. Springer-Verlag, Berlin, pp. 239–275.

Ueno, Y., Yamada, K., Yoshida, N., Maruyama, S., Isozaki, Y., 2006. Evidence from fluid inclusions for microbial methanogenesis in the early Archean era. Nature 440, 516–519.

Volkman, J.K., Alexander, R., Kagi, R.I., Woodhouse, G.W., 1983. Demethylated hopanes in crude oils and their applications in petroleum geochemistry. Geochimica et Cosmochimica Acta 47, 785–794.

Wang, F.Y., Zhang, Z.L., Wu, B.L., Liu, Y.Q., Liu, C.Y., 2005. Diagenesis and formation of a sandstone-type uranium deposit related to hydrocarbon micro-leakage in the northern Ordos basin. Abstracts of the Third China National Meeting of Sedimentology. September 22–24, 2005, Chengdu, China, p. 231.

Watterson, J.R., 1991. Preliminary evidence for the involvement of budding bacteria in the origin of Alaskan placer gold. Geology 20, 315–318.

Widdel, F., Bak, F., 1999. Gram-Negative Mesophilic Sulfate-Reducing Bacteria. Release 3.0. Springer-Verlag, New York. http://141.150.157.117:8080/prokPUB/chaphtm/183/COMPLETE.htm.

Wilhelms, A., Larter, S.R., Head, I., Farrimond, P., di-Primio, R., Zwach, C., 2000. Biodegradation of oil in uplifted basins prevented by deep-burial sterillisation. Nature 411, 1034–1037.

Xiang, W.D., Li, T.G., Fang, X.Y., Chen, X.L., Cheng, H.H., Pang, Y.Q., 2005. Formation characteristics and models of Dongsheng uranium deposit, Ordos basin. Abstracts of the third China National Meeting of Sedimentology. September 22–24, 2005, Chengdu, China, p. 232.

Zhang, C.L., Li, Y.L., Wall, J.D., Larsen, L., Sassen, R., Huang, Y.S., Wang, Y., Peacock, A., White, D.C., Horita, J., Cole, D.R., 2002. Lipid and carbon isotopic evidence of methane-oxidizing and sulfate-reducing bacteria in association with gas hydrates from the Gulf of Mexico. Geology 30, 239–242.

Zhang, L.P., Bai, G.P., Zhao, K.B., Sun, C.Q., 2006. Restudy of acid-extractable hydrocarbon data from surface geochemical survey in the Yimeng Uplift of the Ordos Basin, China: improvement of geochemical prospecting for hydrocarbons. Marine and Petroleum Geology 23, 529–542.